

STAN: Synthetic Network Traffic Generation using Autoregressive Neural Models

Shengzhe Xu¹, Manish Marwah², Naren Ramakrishnan¹
{shengzx@vt.edu, manish.marwah@gmail.com, naren@cs.vt.edu}
¹Department of Computer Science, Virginia Tech, Arlington, USA
²Micro Focus, CA, USA

September 2020

Abstract

Deep learning models have achieved great success in recent years. However, large amounts of data are typically required to train such models. While some types of data, such as images, videos, and text, are easier to find, data in certain domains is difficult to obtain. For instance, cybersecurity applications routinely use network traffic data which organizations are reluctant to share, even internally, due to privacy reasons. An alternative is to use synthetically generated data; however, most existing data generating methods lack the ability to capture complex dependency structures that are usually prevalent in real data by assuming independence either temporally or between attributes. This paper presents our approach called *STAN*, Synthetic Network Traffic Generation using Autoregressive Neural models, to generate realistic synthetic network traffic data. Our novel autoregressive neural architecture captures both temporal dependence and dependence between attributes at any given time. It integrates convolutional neural layers (CNN) with mixture density layers (MDN) and softmax layers to model both continuous and discrete variables. We evaluate performance of *STAN* by training it on both a simulated dataset and a real network traffic data set. Multiple metrics are used to compare the generated data with real data and with data generated via several baseline methods. Finally, to answer the question – can real network traffic data be substituted with synthetic data to train models of comparable accuracy – we consider two commonly used models for anomaly detection in such data, and compare F1/MSE measures of models trained on real data and those on increasing proportions of generated data. The results show only a small decline in accuracy of models trained solely on synthetic data.

1 Introduction

Cybersecurity has become a key concern for both private and public organizations, given the prevalence of cyber-threats and attacks. In fact, malicious cyber-activity cost the U.S. economy between \$57 billion and \$109 billion in 2016 [20], and worldwide yearly spending on cybersecurity reached \$1.5 trillion in 2018 [17].

To gain insights into and counter cybersecurity threats, organizations need to sift through large amounts of network, host and application data typically produced in an organization. Manual inspection of such data by security analysts to discover attacks is impractical due to its sheer volume, e.g., even a medium sized enterprise can produce terabytes of network traffic data in a few hours. Automating the process through use of machine learning tools is the only viable alternative. Recently deep learning models have been successfully used for cyber-security applications [4, 11], and given the large quantities of available data, deep learning methods appear to be a good fit.

However, although large amounts of data is apparently available for cybersecurity machine learning applications, it is sensitive in nature and access to it can result in privacy violations, e.g., network traffic logs can reveal web browsing behavior of users. Thus it is difficult to obtain such data to train models, even internally within an organization. To get around data privacy issues, there are three main approaches [1, 2]: 1) anonymization; 2) cryptographic methods and 3) perturbation methods, such as differential privacy. However, 1) leaks private information in most cases, 2) is usually impractical for large data sets, and 3) degrades data quality making it less suitable for machine learning tasks.

In this paper, we take an orthogonal approach by generating synthetic data that is realistic enough to replace real data in machine learning tasks. Specifically, we consider multivariate time-series data and, unlike prior work, capture both temporal dependence and attributes dependence. Figure 1 illustrates our approach, called *STAN*: Given real historical data, phase 1 trains a CNN-based autoregressive generative neural network that learns joint distribution of data. After the model is trained, phase 2 uses the model to synthesize any amount of synthetic data with the joint distribution of real data without revealing any private information. Phase 3 comprises application of the synthetic data to replace real data in machine learning tasks where model performance¹ is comparable to the model trained on real data.

To evaluate the performance of *STAN*, we use a real publicly available network traffic data set. We compare our method with four selected baselines using several metrics to evaluate the generated data. Finally, we compare the methods on two machine learning tasks – a classification task and a regression task used for detecting cybersecurity anomalies – that are trained on both real and synthetic data. We show a comparable model performance after entirely substituting the real training data with our synthetic data: the F-1 score of the

¹Here performance refers to a model evaluation metric such as precision, recall, F1-score, mean squared error, etc.

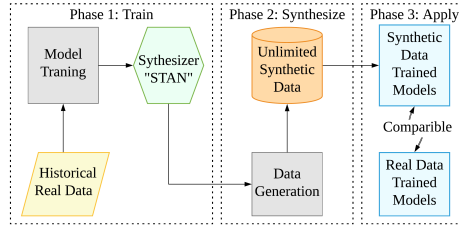


Figure 1: *STAN* consists of three phases: Phase 1 learns a generative model from a given real training data set $D_{Historical}$; Phase 2 uses trained model to sequentially generate synthetic data, D_{Synth} ; Phase 3 use the generated data D_{Synth} , in place of real data D_{Real} , to train machine learning models.

classification task only drops by 4% (78% to 75%), while the mean square error only increases by about 13% for the regression task.

In summary, this paper makes the following key contributions:

- We designed and prototyped *STAN*, a novel tool that learns joint distribution of multivariate time-series data – data typically used in cybersecurity applications – and then generates synthetic data from the learned distribution. Unlike prior work, *STAN* learns both temporal and attribute dependence. Our code is publicly available.²
- *STAN* integrated convolutional neural layers (CNN) with mixture density layers (MDN) and softmax layers to model both continuous and discrete variables.
- We evaluated *STAN* on both simulated data and a real publicly available network traffic data set, and compared with four baselines.
- We build models for two cybersecurity machine learning tasks and showed that while using only *STAN* generated data to train, the performance of the models is comparable to using real data.

2 Related Work

Machine learning for cybersecurity In the past decades, people apply machine learning to multiple tasks in cybersecurity, such as automatically detect malicious activity and stop attacks [6, 7]. Such machine learning approaches usually require a large amount of training data with specific features. However, training model using real user data leads to privacy exposure and ethics problems. Previous work on anonymizing real data [15] has failed to provide satisfactory privacy protection, or degrades data quality too much for machine

²<https://github.com/an-anonymous-repo/ANDS.git>

learning model training. This paper takes a different approach that, by learning and generating realistic synthetic data, the real data can be substituted when training machine learning models.

Synthetic data generation and GAN models Generating synthetic data to make up the lack of real data is a common solution. Compared to modeling image data [13], learning distribution on multi-variate time-series data results in more challenges. Multi-variables data have multiple forms in the real world, so that the data usually have more complex dependency (temporal and spatial) as well as heterogeneous attribute types (continuous or discrete).

Synthetic data generation models often treat each column as a random variable to model joint multivariate probability distributions. The modeled distribution is then used for sampling. Traditional modeling algorithms [3, 9, 18] have the restraint of distribution data types and due to computational issues, the dependability of synthetic data generated by these models is extremely limited. Recently, GANs-based approaches augment performance and flexibility to generate data [14, 21]. However, they are still restricted to a static dependency without considering the temporal dependence usually prevalent in real world data. We are not aware of any prior work that models both temporal and between attributes dependencies.

Autoregressive generative models [13, 19] have been successfully applied to signal data, image data, and natural language data. They attempt to iteratively generate data elements: previously generated elements are used as an input condition for generating the following data. Compared to GAN models, autoregressive models emphasize two factors during the distribution estimating: 1) the importance of the time-sequential factor; 2) an explicit and tractable density. In this paper, we apply the autoregressive idea to learn and generate time-series multi-variable data.

Mixture density networks Unlike modeling discrete attributes, some continuous numeric attributes are relatively sparse and show a large value range. Mixture Density Network [5] presents a neural network architecture to learn a Gaussian mixture model (GMM) that can predict continuous attribute distributions. This architecture provides the possibility to integrate GMM into a complex neural network architecture.

3 Problem Definition

We assume the data to be generated is a multivariate time-series. Specifically, data set \mathbf{x} contains n rows and m columns. Each row $\mathbf{x}_{(i,:)}$ is an observation at time point i and each column $\mathbf{x}_{(:,j)}$ is a random variable j , where $i \in 1..n$ and $j \in 1..m$. Unlike typical tabular data, e.g., that found in relational database tables, and unstructured data, e.g., images, multivariate time-series data poses two main challenges: 1) the rows are generated by an underlying temporal process and are thus not independent, unlike tabular data; 2) the columns or attributes are not necessarily homogeneous, and comprise multiple data types such as numerical, categorical or continuous, unlike say images.

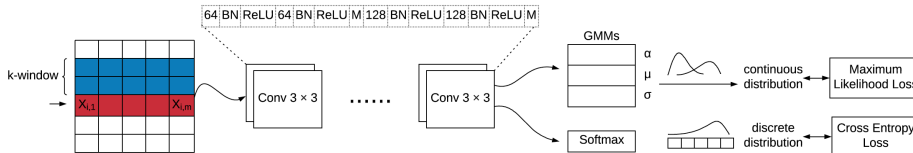


Figure 2: *STAN* components: Left, window CNN, which crops the context based on a sliding window and extracts features from context; Middle, mixture density layers and softmax layers learn to predict the distributions of various types of attributes; Right, the loss functions for different kinds of layers.

The data \mathbf{x} follows an unknown, high-dimensional joint distribution $\mathbb{P}(\mathbf{x})$, which is infeasible to estimate directly. The goal is to estimate $\mathbb{P}(\mathbf{x})$ by a generative model \mathbb{S} which retains the dependency structure across rows and columns. Values in a column typically depend on other columns, and temporal dependence of a row can extend to tens of prior row. Once model \mathbb{S} is trained, it can be used to generate an arbitrary amount of data, \mathbf{D}_{syn} .

Another key challenge is evaluating the quality of the generated data, \mathbf{D}_{syn} . Assuming a data set, $\mathbf{D}_{historical}$, is used to train \mathbb{S} , and an unseen test data set, \mathbf{D}_{test} , is used to evaluate the performance of \mathbb{S} , we use two criteria to compare \mathbf{D}_{syn} with \mathbf{D}_{test} : 1) similarity between a metric M evaluated on the two data sets, that is $M(\mathbf{D}_{test}) \approx M(\mathbf{D}_{syn})$ 2) similarity between performance P on training the same machine learning task T , in which the real data, \mathbf{D}_{test} , is replaced by the synthetic data, \mathbf{D}_{syn} , that is $P[T(\mathbf{D}_{test})] \approx P[T(\mathbf{D}_{syn})]$.

4 Proposed Method

We model the joint data distribution, $\mathbb{P}(\mathbf{x})$, using an autoregressive neural network. The model architecture, shown in Figure 2, combines CNN layers with a density mixture network [5]. The CNN captures temporal and spatial (between attributes) dependencies, while the density mixture layer uses the learned representation to model the joint distribution. During the training phase, for each row, *STAN* takes a data window prior to it as input. Given this context, the network learns the conditional distribution for each attribute. Both continuous and discrete attributes can be modeled. While a density mixture layer is used for continuous attributes, a softmax layer is used for discrete attributes.

In the synthesis phase, *STAN* sequentially generates each attribute in each row. Every generated attribute in a row, having been sampled from a conditional distribution over the prior context, serves as the next attribute’s context.

4.1 Joint distribution factorization

$\mathbb{P}(\mathbf{x})$ denotes the joint probability of data \mathbf{x} composed of n rows and m attributes. We can expand the data as a one-dimensional sequence $\mathbf{x}_1, \dots, \mathbf{x}_n$, where each vector \mathbf{x}_i represents one row including the m attributes $x_{i,1}, \dots, x_{i,m}$.

To estimate the joint distribution $\mathbb{P}(\mathbf{x})$ we write it as the product of conditional distributions over the rows. We start from the joint distribution factorization with no assumptions:

$$\mathbb{P}(\mathbf{x}) = \prod_{i=1}^n \mathbb{P}(\mathbf{x}_i | \mathbf{x}_1, \dots, \mathbf{x}_{i-1}) \quad (1)$$

Unlike unstructured data such as images, multivariate time-series data usually corresponds to underlying continuous processes in the real world and do not have an exact starting and ending points. It is impractical to make a row probability $\mathbb{P}(\mathbf{x}_i)$ depend on all prior rows as in Equation 1. Thus, a k -sized sliding window is utilized to restrict the context to only the k most recent rows. In other words, a row conditioned on the past k rows is independent of all remaining prior rows, that is, for $i > k$, we assume independence between \mathbf{x}_i and $\mathbf{x}_{<i-k}$. We can thus rewrite the joint distribution $\mathbb{P}(\mathbf{x})$ as the product of the conditional distributions over the prior k rows:

$$\mathbb{P}(\mathbf{x}) = \prod_{i=1}^k \mathbb{P}(\mathbf{x}_i | \mathbf{x}_1, \dots, \mathbf{x}_{i-1}) \prod_{i=k+1}^n \mathbb{P}(\mathbf{x}_i | \mathbf{x}_{i-k}, \dots, \mathbf{x}_{i-1}) \quad (2)$$

Note that a suitable value of k needs to be picked based on empirical evidence or domain knowledge. While all the probabilities in the second term on the RHS of Equation 2 are conditioned on k variables, the same is not true for the probabilities in the first term. To make these consistent, we add zero padding and then symbolically define that \mathbf{x}_i where $i \leq 0$ represents a padding row, as Equation 3 shows.

$$\begin{aligned} \mathbb{P}(\mathbf{x}) &= \prod_{i=1}^k \mathbb{P}(\mathbf{x}_i | \mathbf{x}_{i-k}, \dots, \mathbf{x}_1, \dots, \mathbf{x}_{i-1}) \prod_{i=k+1}^n \mathbb{P}(\mathbf{x}_i | \mathbf{x}_{i-k}, \dots, \mathbf{x}_{i-1}) \\ &= \prod_{i=1}^n \mathbb{P}(\mathbf{x}_i | \mathbf{x}_{i-k}, \dots, \mathbf{x}_{i-1}) \end{aligned} \quad (3)$$

The joint distribution of a row can be factorized in two ways: 1) Equation 4 assumes conditional independence of attributes in a row, given all attributes in the previous k rows; 2) Equation 5 makes no conditional independence assumptions of attributes in the same row.

$$\mathbb{P}(\mathbf{x}) = \prod_{i=1}^n \prod_{j=1}^m \mathbb{P}(\mathbf{x}_{i,j} | \mathbf{x}_{i-k}, \dots, \mathbf{x}_{i-1}) \quad (4)$$

$$\mathbb{P}(\mathbf{x}) = \prod_{i=1}^n \prod_{j=1}^m \mathbb{P}(\mathbf{x}_{i,j} | \mathbf{x}_{i-k}, \dots, \mathbf{x}_{i-1}; x_{i,1}, \dots, x_{i,j-1}) \quad (5)$$

While (4) provides a good approximation, we found (5) performs slightly better.

4.2 Neural network architecture

As shown in Figure 2, the input window goes through the *convolutional layers* followed by *mixture density layers* or *softmax layers* sequentially to learn the joint distribution. We define two *loss* functions for the two distribution modeling layers separately. Algorithms 1 and 2 provide details on model training and data synthesis. Note that the training phase allows for parallelization while the synthesis phase is sequential.

Algorithm 1 Model Training process for each attribute j

Input $D_{Historical}$, window size k , attribute type T_j .

Output STAN model \mathbb{S}_{stan} ;

- 1: Construct window data
 - $X_i^{window} = \text{concatenate } X_{i-k}, \dots, X_{i-1}$;
 - $y_i^{window} = X_i$;
 - 2: **for** epoch in 1 ... EPOCH **do**
 - 3: $X_i^{window} *= Mask$
 - 4: **if** T_j is continuous **then**
 - 5: $\mathbb{P}_{gmm_pred} = mdn(wcnn(X_{window}))$;
 - 6: $loss = nll(\mathbb{P}_{gmm_pred}, y_{window})$;
 - 7: **else**
 - 8: $\mathbb{P}_{softmax_pred} = softmax(wcnn(X_{window}))$;
 - 9: $loss = cross_entropy(\mathbb{P}_{softmax_pred}, y_{window})$;
 - 10: **end if**
 - 11: Update \mathbb{S}_{stan} with $loss$;
 - 12: **end for**
-

Algorithm 2 Data Synthesis process

Input Trained STAN model \mathbb{S}_{stan} .

Output D_{synth} ;

- 1: Init context $X^{window} = \text{marginal sampling}()$
 - 2: **while** condition(target row number or time stamp) **do**
 - 3: $X_i^{window} *= Mask$
 - 4: $P_{pred} = \mathbb{S}_{stan}(X_i^{window})$;
 - 5: $y_{sample} = \text{sample from distribution } \mathbb{P}_{pred}$;
 - 6: $X_{i+1}^{window} = X_i^{window}[1 :, :] + y_{sample}$
 - 7: **end while**
-

Window convolutional layers (wcnn). The CNN layers which we call window CNN since they operate on a sliding window of data, perform a two-dimensional convolution. For one row \mathbf{x}_i the layers capture a rectangular context above the row as shown in Figure 2. *STAN* uses multiple convolutional layers that preserve the spatial and temporal resolution in a sliding time window box, each number in Figure 2 represents the number of $3 * 3$ filters in that layer.

Batchnorm, ReLU and max pooling layers are also used, marked as *BN*, *ReLU*, and *M*, respectively.

Convolution mask Based on which factorization is selected, we have mask A for Equation 4 and mask B for Equation 5.

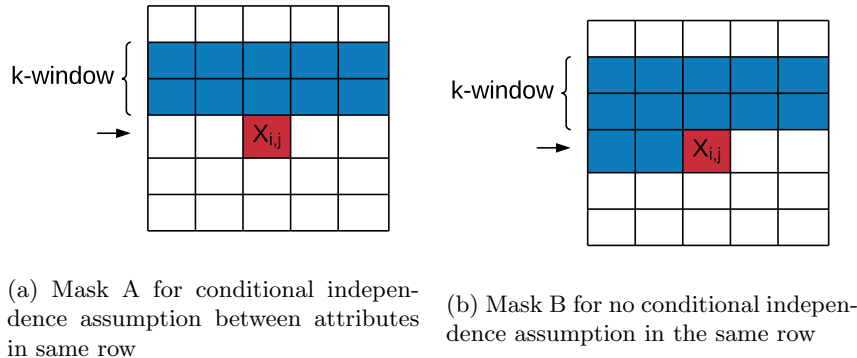


Figure 3: Masks for context window convolution

Mixture density layer (mdn) learns a conditional *gaussian mixture distribution*. It consists of three parallel fully connected layers, modeling $\alpha_i, \sigma_i, \mu_i$ separately, where the parameter α_i represents for the component weights of an *gaussian mixture model*, and the μ_i and σ_i^2 are the mean and variance parameters of the gaussian distribution components. The α_i parameters output go to a softmax, so that the weights of all the Gaussian mixture components sum to one.

Loss functions We define loss functions for *mixture density layer* and *softmax layer* separately. Note that the two losses have different scales, and while multitask learning has its advantages, we match each *mixture density component* or *softmax component* with an individual *wcnn component*.

Negative Log-Likelihood Loss (NLL) is used for the mixture density layers, which predict a group of mixture density parameters that can compose a Gaussian mixture model as Equation 6: $\alpha_i, \sigma_i, \mu_i$. We use maximum likelihood loss to estimate a true distribution: the label of the input, which is the new row that to be generated, is supposed to have the highest probability in the estimated distribution. Cross entropy loss is used for the softmax layer.

$$NLL(x|\mu, \sigma^2) = -\log \sum \alpha_i * \mathcal{N}(x|\mu_i, \sigma_i^2) \quad (6)$$

4.3 Baselines

We selected four different methods to serve as baselines for our method. This range for basic Gaussian Mixture Model, Bayesian Network to two recent deep learning approaches that use GANs for synthetic data generation, which for

brevity we refer to as B1, B2, B3, and B4, respectively. We compare *STAN* with these baselines and analyze the distribution factorization.

Gaussian Mixture (B1) This assumes all attributes at a particular time step are independent of each other, and further each row is independent. Thus it can be factorized as following:

$$\mathbb{P}(\mathbf{x}) = \prod_{i=1}^n \mathbb{P}(\mathbf{x}_i) \quad (7a) \qquad \mathbb{P}(\mathbf{x}_i) = \prod_{j=1}^m \mathbb{P}(\mathbf{x}_{i,j}) \quad (7b)$$

Bayesian Network (B2) As a traditional statistical approach, limited temporal or attributes dependence can be learnt based on the domain knowledge from experts. For example, if \mathbf{x}_{i,j_1} is dependent on \mathbf{x}_{i-1,j_1} and \mathbf{x}_{i,j_2} , we can write it as a product of the conditional distributions (see Equation 8). The value $\mathbb{P}(\mathbf{x}_{i,j_1} | \mathbf{x}_{i-1,j_1}, \mathbf{x}_{i,j_2})$ is the probability of the j_1 attributes of the i -th observation row, given the $(i-1)$ -th j_1 attribute and the i -th j_2 attribute. Considering the edge situation as well as utilizing the Bayes rule, we rewrite the distribution $\mathbb{P}(\mathbf{x}_{i,j_1} | \mathbf{x}_{i-1,j_1}, \mathbf{x}_{i,j_2})$ as:

$$\begin{aligned} \mathbb{P}(\mathbf{x}) &= \prod_{i=1}^n [\mathbb{P}(x_{i,j_1} | x_{i,j_2}, x_{i-1,j_1}) \prod_{j=1, j \neq j_1}^m \mathbb{P}(x_{i,j})] \\ &= \mathbb{P}(x_1) \cdot \prod_{i=2}^n [\mathbb{P}(x_{i,j_1}) \mathbb{P}(x_{i-1,j_1} | x_{i,j_1}) \mathbb{P}(x_{i,j_2} | x_{i,j_2})] \\ &\quad \cdot \prod_{j=1, j \neq j_1}^m \mathbb{P}(x_{i,j}) \end{aligned} \quad (8)$$

WP-GAN (B3) [16] utilizes GAN to specifically generate network traffic flow data, while **CTGAN (B4)** [21] utilizes GAN to generate general tabular data which contains both discrete and continuous attributes. Both B3 and B4 assume attribute dependence at a certain time step but ignore temporal-wise dependence. Thus the joint distribution can be factorized as Equation 7a only, while the factorization inside each row is untractable due to the GAN mechanism.

4.4 Evaluation Metrics

The evaluation of generative models is challenging and subjective. We use multiple metrics to compare them: likelihood, distribution evaluation, domain knowledge rule test, and machine learning tasks performance comparison.

Likelihood fitness The likelihood function measures the goodness of a statistical model fitting a data sample. However, the intrinsic difference between explicit density method (B1, B2, and *STAN*) and implicit density method (B3

and B4) makes it more challenging to compare them. [8] also claims that there is not a fair way to directly compare the likelihood of the GAN models. Thus in this paper, we only compare the likelihood between explicit density models: B1, B2 and, *STAN*.

Distribution and JS divergence Although the goal of our work is to model joint distribution of a window of data, we also compare the marginal distributions of the individual attributes. As a quantitative metric, we calculate Jensen-Shannon divergence between the distributions of the generated data \mathbf{D}_{syn} and the real data \mathbf{D}_{test} in each attribute.

Domain knowledge test We use domain knowledge checks to evaluate the synthetic data quality. Since the application data set pertains to network traffic flow, we use several properties that such data need to satisfy in order to be realistic.[16]

Machine learning application task The final goal of generating synthetic data is to build machine learning models without using any real data. To evaluate whether the generated data is able to replace real data in a model training process, we select two tasks that are used in cybersecurity anomaly detection. One is a classification task while the other is regression. Both are self-supervised tasks.

The first task is predicting the protocol field in the network traffic data, while the second task is to predict the number of bytes field. In practice once trained these models are used for marking anomalies when the actual value significantly differs from the real one. We train a RandomForest model for the classification task, and a neural network model for the regression task. For both tasks we compare the cross-validation performance of the models trained on real and synthetically generated data.

5 Experimental Results

To demonstrate its effectiveness, we train and evaluate *STAN* on a real network traffic data set. However, initially to experiment with some architectural variations, we use a simple simulated data set.

5.1 Simulated data

We built a simulated data set with a simple random process whose dependence can be clearly controlled. We simulated a two-variable data distribution with the following formula and sampled 10,000 points data set (X, Y) from it: $x_i = 0.9x_{i-1} + 0.1\mathcal{N}$ and $y_i = 0.9x_i + 0.1\mathcal{N}$, where \mathcal{N} is standard normal distribution noise.

We apply a naive version *STAN*, that passes through the input to mixture density layers directly, and B1 on the simulated data set. We evaluated the correlation coefficient R between both temporal dependence $R(X_i, X_{i-1})$ and attribute dependence $R(X_i, Y_i)$. Figure 4 presents the scatter plots of x_i and y_i that from four data source (both raw simulated data and synthetic data).

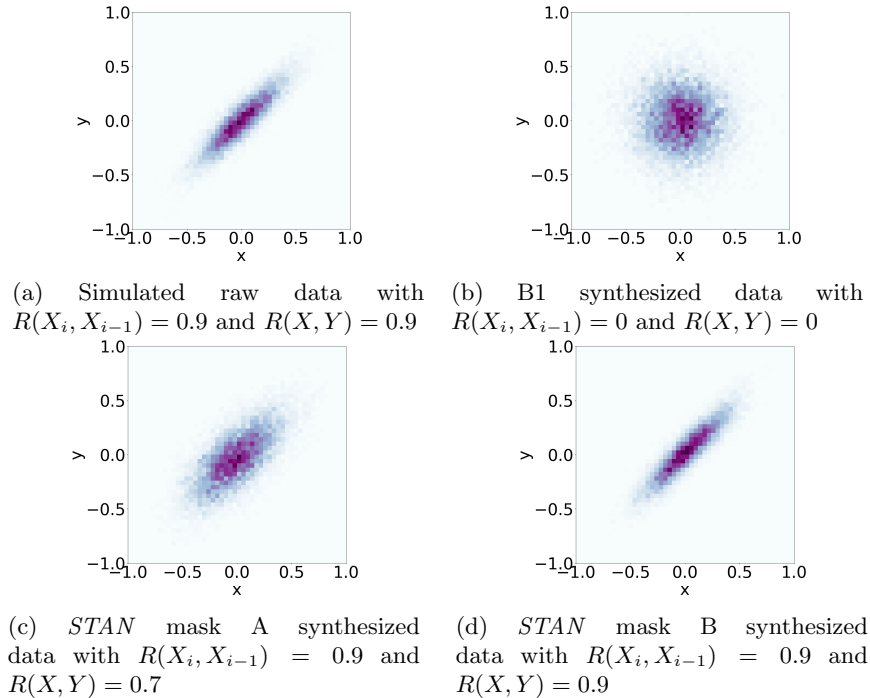


Figure 4: (X_i, Y_i) scatter plot of the simulated data and synthetic data with the Correlation Coefficients R .

Observation 1: *Same-row attribute conditional independence provides a reasonable approximation*

5.2 Real network traffic data

Data set Network traffic data is typically a multivariate time-series. A common format is called *netflow*, where each row represents a unidirectional network traffic connection or flow. We selected a netflow data set for our experiments as a large data set was publicly available, and further because it is a good representative format for network traffic data in general. Typically each row consists of the following attributes: timestamp at the end of a flow (te), duration of flow (td), packets exchanged in the flow (pkt), and the corresponding number of bytes (byt), source IP address (sa), destination IP (da) and protocol (pr). So one row x_i can be expressed as a tuple of $(te_i, byt_i, sa_i, da_i, pr_i, \text{etc})$. Table 1 shows typical attributes, their types and examples.

We apply *STAN* on a publicly available benchmark netflow data set, UGR’16 [12], which contains large scale traffic data captured by a Tier-3 ISP cloud service provider. First, we randomly select the April week3 data to focus on. Second, we randomly select 90 users based on the number of traffic flows per user

| Attribute | Type | Example |
|--------------------|-------------|---------------------|
| timestamp | continuous | 2016-04-11 00:02:15 |
| duration | continuous | 0.344 |
| transport protocol | categorical | TCP |
| source IP address | categorical | 85.201.196.53 |
| source port | categorical | 19925 |
| dest. IP address | categorical | 42.219.145.151 |
| dest. port | categorical | 80 |
| bytes | numeric | 11238 |
| packets | numeric | 11 |

Table 1: Overview of typical attributes in flow-based data.

distribution. Third, we extract one day’s (Monday) data to be the $\mathbf{D}_{historical}$ and another day (Tuesday) of the same user group and the same week to be the \mathbf{D}_{test} . Lastly, from a cybersecurity perspective, we are most interested in users with traffic between an organization and external IP addresses rather than traffic within an organization. Following this strategy, we selected 1,531,126 samples for the $\mathbf{D}_{historical}$ and 1,952,702 samples for the \mathbf{D}_{test} .

Pre-processing To ensure the trained model is a practical and robust tool to synthesize network traffic flow data, we normalize the raw netflow data so that the neural network can deal with it. Also, the neural network predicted variable value could also be interpreted back to the original form. Since it is just a regular data processing trick, we provide details in supplemental materials.

Likelihood For each data point (each row), we can directly calculate the row likelihood by factorization Equations 4, 5 and 7b. Take the attribute *byt* for example the negative log likelihood evaluated on the UGR16 validation set for B1, B2 and *STAN* are 4.85, 3.90, 2.34 respectively. More attribute likelihood table in the appendix show *STAN* is the best reported over all the comparable attributes, including continuous and discrete attributes.

Distribution and JS divergence Figure 5 shows the individual JS divergence of the marginal distribution of both the continuous and discrete attributes. *STAN* captures the marginal distribution well for most attributes. Even though B1 precisely models the marginal distribution of the training data set, it does not perform as well as *STAN* on the test data set. We believe this is because the marginal distribution over a day is non-stationary.

Observation 2: *STAN models the marginal distribution better than baseline B1.*

Domain knowledge test We employ domain test developed by [16] for netflow data. These are several rules that need to be satisfied by generated flow-based network data. We highlight three tests here which are summarized in Table 2. *STAN* performs well in all three:

- Test 1: The selected UGR16 data set is captured by an ISP. Therefore, at least one IP address (source IP address or destination IP address) of each

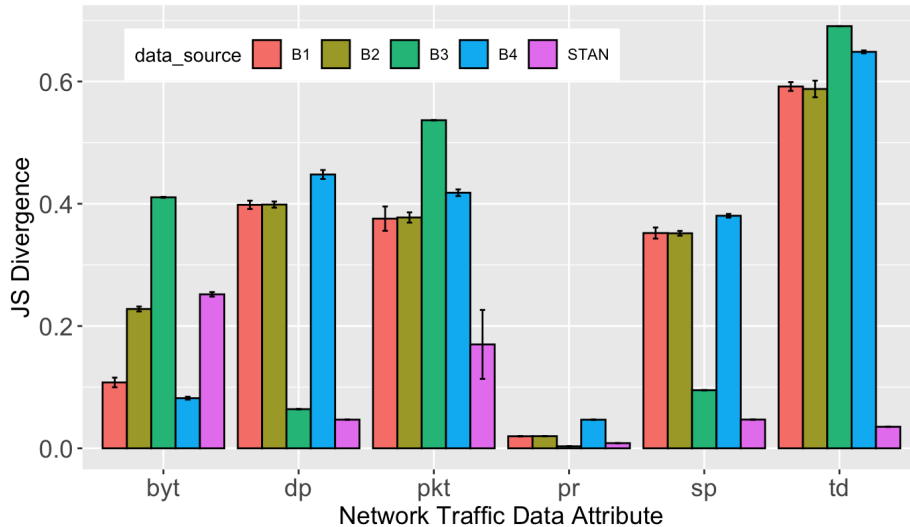


Figure 5: JS divergence between attribute marginal distribution of real and synthetic data

flow must belong to the ISP (starting with 42.219.XXX.XXX).

- Test 2: If the flow describes normal user behavior and the source port or destination port is 80 (HTTP) or 443 (HTTPS), the transport protocol must be TCP.
- Test 3: TCP and UDP packets have a minimum and maximum packet size. Therefore, we check the relationship between bytes and packets in each flow according to the following rule: $42 \cdot \text{packets} \leq \text{bytes} \leq 65535 \cdot \text{packets}$.

| | Test 1 | Test 2 | Test 3 |
|-------------|------------|-----------|-----------|
| Real Data | 100 | 100 | 94 |
| B1 | 69 | 77 | 51 |
| B2 | 69 | 78 | 50 |
| B3 [16] | 99 | 99 | 79 |
| B4 [21] | 92 | 99 | 75 |
| <i>STAN</i> | 100 | 99 | 81 |

Table 2: Passing percentage of domain knowledge tests

Real application tasks Finally, we test our synthetic data on two cybersecurity machine learning applications – one is a classification task, and the other is regression. The goal is to figure out whether it is possible to fully substitute real data with synthetic data for training machine learning models.

A series of models are trained on real test data. We start our training from using a complete \mathbf{D}_{test} (real data) and successively decrease the amount of real data until no data from \mathbf{D}_{test} is used. Another series of models are trained similarly using the real test data; however, instead of simply removing certain amount of data from \mathbf{D}_{test} , we substitute the indicated amount of data with our synthetic data \mathbf{D}_{syn} , so that the total amount of data is kept unchanged.

In the following two tasks, we use \mathbf{D}_{test} , which is unseen and never used in the synthesizer training process. For the synthetic data \mathbf{D}_{synth} , every synthesizer model generates five sets of synthetic data sample, so we can compute error bars. Five-fold cross validation is used to get a robust estimate of the measurements.

Task1: protocol forecasting Fig. 6 shows the F-1 scores achieved by Random Forest models. There are six sets of models. 'Real-Data': these are random forest models trained by reducing the real data; 'stan': these are random forest models trained by reducing the real data, but substituting the reduced data by synthetic data generated by *STAN*; 'B1' through 'B4': these are similar to the 'stan' models but obtained by substituting the reduced data by the four baselines respectively. The x-axis represents how much real data is used from 100% down to 0%.

If we only use real data, the F1 score drops from 0.78 down to 0.6 as the amount of data decreases. Clearly, with no real data, we are unable to train a model. When we substitute real data with that generated by the baselines, the performance drops even quicker, because they do a poor job of capturing the temporal and attribute dependence. Even in the absence of any real data, data generated by *STAN* results in an F1 score of 0.75, where the drop in performance is only 4%. That is, the model built with only synthetic data retains 96% of the performance of the all real data trained model.

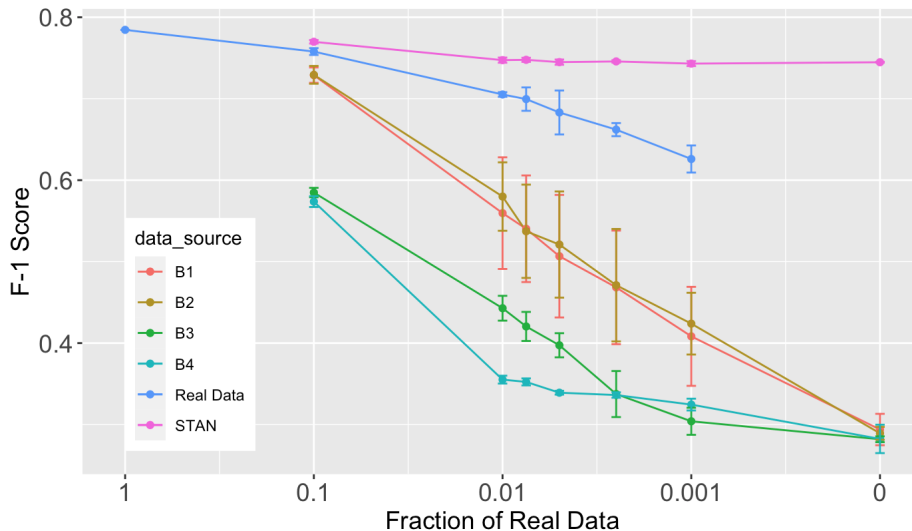


Figure 6: F1-score of Protocol Forecasting Task

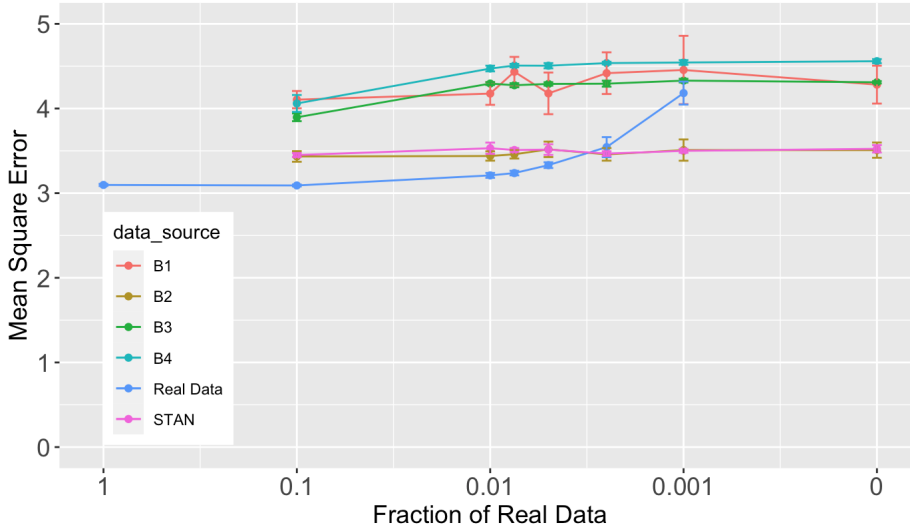


Figure 7: Mean Square Error of *byt* Value Forecasting Task

Task2: *byt* value forecasting follows a similar setup of experiments as Task1. Fig. 7 shows the mean square error achieved by a neural network regression model. The plot shows that *STAN* and Bayesian network (B2) outperform the other three baseline models. Building a Bayesian network with domain knowledge typically performs better than GANs [21].

Observation 3: *Comparing to B2, STAN can still get the same performance even without domain knowledge.*

In our experiments, B2 is optimized specifically for the *byt* sequential value. However, *STAN* has two advantages over the Bayesian network. First, users do not need the domain knowledge required for Bayesian network implementation. Secondly, there is no inherent bias attributable to an expert unlike traditional Bayesian networks. Similar to the first task, the penalty for using only *STAN* generated data (with no real data) is low, an increase of 13% in the mean square error.

Observation 4: *Even with 0% real data, STAN models task1 and task2 with only a small drop in accuracy.*

6 Conclusion

This paper presents the design and implementation of *STAN*, a novel, flexible and robust approach to learn the distribution of complex multivariate time-series data distributions. Compared to existing approaches, *STAN* is novel in several aspects. First, *STAN* learns the joint distribution over both temporal dependency and attribute dependency. Second, *STAN* is flexible to generate data with any combination of continuous and discrete attributes. Furthermore,

we perform a thorough evaluation of *STAN* comparing it with four baselines and using several performance measures as well as two cybersecurity machine learning tasks.

Our future work includes building techniques to (1) build complete system of learning and generating network traffic data, (2) explore the best updating rate for re-learning the data synthesizer on the historical data $\mathbf{D}_{\text{historical}}$ (3) conduct more semantic or statistic checking with regards to the fungibility of synthetic data with real data.

References

- [1] Charu C. Aggarwal and Philip S. Yu. *A General Survey of Privacy-Preserving Data Mining Models and Algorithms*, pages 11–52. Springer US, Boston, MA, 2008.
- [2] Mohammad Al-Rubaie and J Morris Chang. Privacy-preserving machine learning: Threats and solutions. *IEEE Security & Privacy*, 17(2):49–58, 2019.
- [3] Laura Aviñó, Matteo Ruffini, and Ricard Gavaldà. Generating synthetic but plausible healthcare record datasets. *arXiv preprint arXiv:1807.01514*, 2018.
- [4] Daniel S Berman, Anna L Buczak, Jeffrey S Chavis, and Cherita L Corbett. A survey of deep learning methods for cyber security. *Information*, 10(4):122, 2019.
- [5] Christopher M Bishop. Mixture density networks. 1994.
- [6] Anna L Buczak and Erhan Guven. A survey of data mining and machine learning methods for cyber security intrusion detection. *IEEE Communications surveys & tutorials*, 18(2):1153–1176, 2015.
- [7] Carlos A Catania and Carlos García Garino. Automatic network intrusion detection: Current techniques and open issues. *Computers & Electrical Engineering*, 38(5):1062–1072, 2012.
- [8] Ian Goodfellow, Jean Pouget-Abadie, Mehdi Mirza, Bing Xu, David Warde-Farley, Sherjil Ozair, Aaron Courville, and Yoshua Bengio. Generative adversarial nets. In *Advances in neural information processing systems*, pages 2672–2680, Cambridge, MA, USA, 2014. MIT Press.
- [9] Cormode Graham. Differentially private spatial decompositions. In *Data engineering (ICDE), 2012 IEEE 28th international conference*, 2012.
- [10] Diederik P Kingma and Jimmy Ba. Adam: A method for stochastic optimization. *arXiv preprint arXiv:1412.6980*, 2014.

- [11] Donghwoon Kwon, Hyunjoo Kim, Jino Kim, Sang C Suh, Ikkyun Kim, and Kuinam J Kim. A survey of deep learning-based network anomaly detection. *Cluster Computing*, pages 1–13, 2017.
- [12] Gabriel Maciá-Fernández, José Camacho, Roberto Magán-Carrión, Pedro García-Teodoro, and Roberto Therón. Ugr '16: A new dataset for the evaluation of cyclostationarity-based network idss. *Computers & Security*, 73:411–424, 2018.
- [13] Aaron van den Oord, Nal Kalchbrenner, and Koray Kavukcuoglu. Pixel recurrent neural networks. *arXiv preprint arXiv:1601.06759*, 2016.
- [14] Noseong Park, Mahmoud Mohammadi, Kshitij Gorde, Sushil Jajodia, Hongkyu Park, and Youngmin Kim. Data synthesis based on generative adversarial networks. *Proceedings of the VLDB Endowment*, 11(10):1071–1083, 2018.
- [15] Shukor Razak, Nur Hafizah, and Arafat Al-Dhaqm. Data anonymization using pseudonym system to preserve data privacy. *IEEE Access*, 2020.
- [16] Markus Ring, Daniel Schlör, Dieter Landes, and Andreas Hotho. Flow-based network traffic generation using generative adversarial networks. *Computers & Security*, 82:156–172, 2019.
- [17] RiskiqInc. The evil internet minute 2019, <https://www.riskiq.com/infographic/evil-internet-minute-2019>, 2019.
- [18] Yi Sun, Alfredo Cuesta-Infante, and Kalyan Veeramachaneni. Learning vine copula models for synthetic data generation. In *Proceedings of the AAAI Conference on Artificial Intelligence*, volume 33, pages 5049–5057, 2019.
- [19] Aaron Van den Oord, Nal Kalchbrenner, Lasse Espeholt, Oriol Vinyals, Alex Graves, et al. Conditional image generation with pixelcnn decoders. In *Advances in neural information processing systems*, pages 4790–4798, 2016.
- [20] WhiteHouse. The cost of malicious cyber activity to the u.s. economy, 2018.
- [21] Lei Xu, Maria Skoularidou, Alfredo Cuesta-Infante, and Kalyan Veeramachaneni. Modeling tabular data using conditional gan. In *Advances in Neural Information Processing Systems*, pages 7333–7343, 2019.

7 Appendix: Simulated data

7.1 Quantitative Metric

We evaluated the correlation coefficient R between both temporal dependence $R(X_i, X_{i-1})$ and attribute dependence $R(X_i, Y_i)$. Figure 8 presents the scatter plots of X_i and X_{i-1} from four data sources (simulated data, B1 synthetic data, *STAN* with mask A synthetic data, and *STAN* with mask B synthetic data), and Figure 9 presents that for X_i and Y_i . Since mask A and mask B represent *conditional independence* and *explicit dependence* respectively, we summarize through this observation,:

- Both conditional independence and explicit dependence provide reasonable approximation on temporal dependence. The $R(X_i, X_{i-1})$ of simulated data, *STAN* mask A, and *STAN* mask B are 0.9.
- Conditional independence provides a reasonable same-row attribute approximation, while explicit dependence performs better. The $R(X_i, Y_i)$ of simulated data, and *STAN* mask B are 0.9; while that of *STAN* mask A is 0.7.

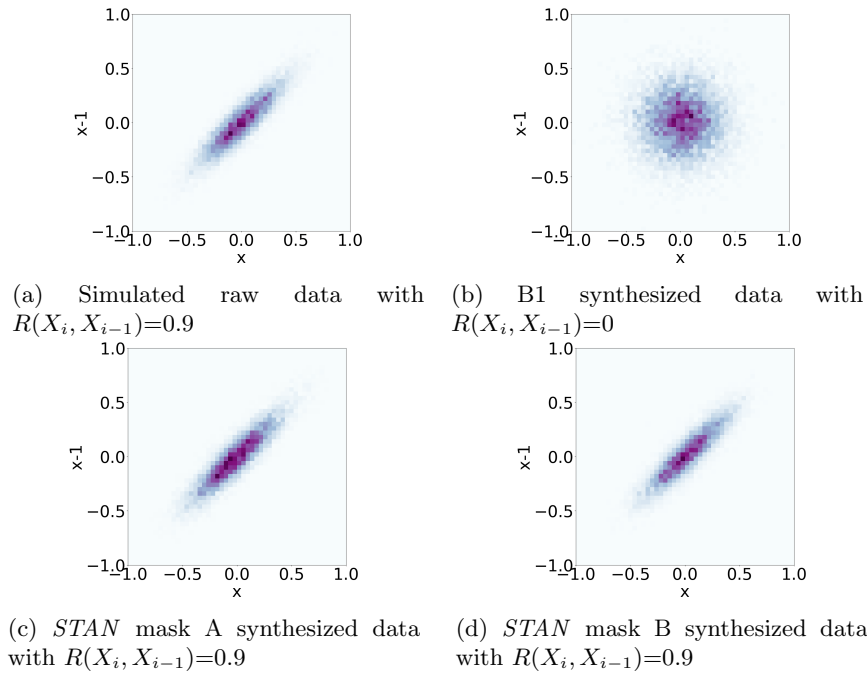


Figure 8: (X_i, X_{i-1}) scatter plot of the simulated data and synthetic data with the Correlation Coefficients R .

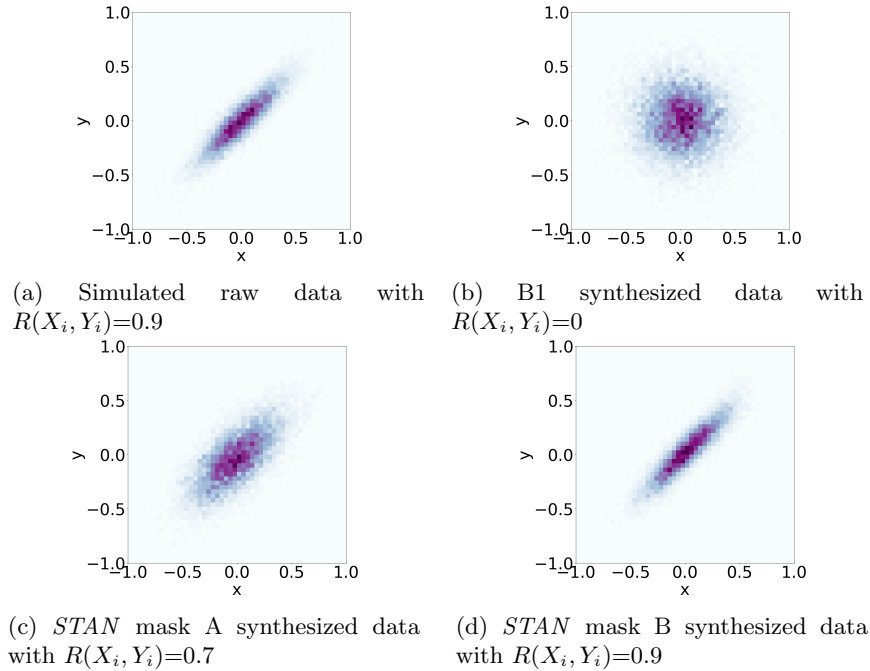


Figure 9: (X_i, Y_i) scatter plot of the simulated data and synthetic data with the Correlation Coefficients R .

7.2 Machine Learning Task

We also used the simulated data and the corresponding synthetic data for training two machine learning tasks (using scikit-learn Python library). In these experiments, we trained the models with different synthetic data or the simulated data and test the model performance (Mean Square Error) on the simulated test data.

- **T1:** predict y_i given x_i (row attribute dependence).
- **T2:** predict x_{i+1} given x_i (temporal dependence).

Table 3 shows that a machine learning model trained only on synthetic data generated by *STAN* produces similar test loss as that trained on real simulated test data.

| Training Data | MSE(T1) | MSE(T2) |
|----------------|------------------|------------------|
| Simulated data | 0.010 | 0.01 |
| B1 | 0.050 | 0.05 |
| STAN mask A | 0.013 | 0.01 |
| STAN mask B | 0.010 | 0.01 |

Table 3: Mean Square Error of the two tasks

8 Appendix: *STAN* Model on UGR16 Netflow data

8.1 Training Hyperparameter

Our models are trained on four Tesla P100 GPUs using the Pytorch toolbox. From the different parameter update rules tried, Adam [10] gives best convergence performance and is used for all experiments. The learning rate schedules were manually set to the highest values that allowed fast convergence: 0.001 for gaussian mixture layers and 0.01 for softmax layers. The batch sizes are also manually set for the experiments. For UGR16, we use as large a batch size as that permitted quick converge; this corresponds to 512 time windows input per batch. We use preprocessing to prepare data batches that can be trained in parallel and accelerate the training and generation process. For the initial convolution network layer parameters, we sample from a Uniform distribution.

8.2 Data Pre-processing

The inputs to the neural model are pre-processed to facilitate training. The numerical attributes are min-max scaled, for the categorical attributes, we apply one-hot encoding. Specifically, for the protocol attribute we use a three-way softmax (for TCP, UDP and other). For source and destination port number attributes, we handle well-known and other ports differently; port up to 1024 are one-hot encoded with softmax output, while higher ports are modeled as a numeric attribute. Instead of modeling timestamps of individual flows, we model the time deltas between them.

8.3 Likelihood

For each data point (each row), we can directly calculate the row likelihood by factorization equations. In our case, explicit density generative models (B1, B2 and *STAN*) clearly define the distribution for each attributes and for those we can evaluate the modeled distribution directly via individual attribute distribution. For a more straightforward form, we use a 200 bin size for continuous variables to validate their negative log-likelihood value for all the baselines and attributes, based on the variable value range and the data set size. In Table 4

Table 4: Attribute negative log likelihood of models evaluated on the UGR16 validation set

| Model | bytes | packet | time duration | protocol |
|-------------|-------|--------|---------------|----------|
| B1 | 4.85 | 3.78 | 1.81 | 0.341 |
| B2 | 3.90 | 2.62 | 0.97 | 0.344 |
| <i>STAN</i> | 2.34 | 1.73 | 0.59 | 0.002 |

we report the negative log likelihood of a few attributes as modelled by *STAN* and baselines B1 and B2. *STAN* produces better results for both continuous and discrete attributes.